Transactions Letters

Performance of Filter Bank Modulation with Phase Noise

Nicola Moret, *Student Member, IEEE,* and Andrea M. Tonello, *Member, IEEE*

***Abstract*—We study the effect of phase noise in filter bank modulation systems. In particular, we analyze the FMT (Filtered Multitone) and the DMT (Discrete Multitone) system. While DMT uses a rectangular shape sub-channel pulse, the FMT system uses a frequency confined pulse. Approximated symbol error rate expressions for M-PSK and M-QAM constellations are derived for two types of receivers: the non-coherent receiver, and the one-tap coherent receiver. The results show that FMT with a root-raised-cosine pulse has some more robustness to phase noise w.r.t. DMT, although both systems are affected by phase noise especially with high order modulation.**

***Index Terms*—DMT modulation, FMT modulation, Phase Noise, Common Phase Error, OFDM.**

I. Introduction

We study the effect of phase noise due to non ideal oscillators in filter bank (FB) modulation systems. In particular, we analyze the FMT (Filtered Multitone) system [1]-[2] and the DMT (Discrete Multitone) system that is also referred to as orthogonal frequency division multiplexing (OFDM) [3]. FMT is a discrete-time implementation of multi-carrier modulation that uses uniformly spaced sub-carriers and identical sub-channel pulses. DMT can be viewed as an FMT scheme that deploys rectangular time domain filters. While DMT privileges the time confinement of the sub-channel pulse, in FMT the pulse design privileges the frequency confinement. For instance, a root-raised-cosine pulse, or customly designed low pass finite impulse response filters [4], or short duration orthogonal pulses [5], can be used in FMT.

Although FB modulation systems are robust to channel frequency selectivity, they are sensitive to fast channel time variations [6], as well as to carrier frequency offsets and phase noise (PN). An extensive literature exists on the performance analysis of multicarrier systems in the presence of phase noise, e.g., [7]-[11]. However, at the best of our knowledge, most of the work considers the DMT scheme where the phase noise introduces a phase shift on the signal of interest often referred to as CPE, as well as inter-channel (ICI) interference due to the loss of sub-channel orthogonality. In [7]-[8] the authors focus on the CPE effects and analyze the performance considering a one-tap equalizer. In [9] the ICI component is also considered and an approach for its mitigation is proposed. Some early work on the capacity comparison between DMT and FMT in the presence of PN was done in [10] although it was limited to simulation results. Preliminary error rate comparisons of DMT and FMT with PN were reported in [11].

In this letter, we provide a general framework to the analysis of the CPE and the interference components, i.e., the inter-symbol interference (ISI) and the ICI, in FB modulation. We focus the analysis on the FMT and DMT systems. We propose approximated expressions of the symbol error rate for M-PSK and M-QAM constellations with both a non-coherent and a one-tap coherent receiver (equalizer), using a stationary model for the PN impairment process and under the Gaussian interference assumption. Several simulation results are reported to validate the theoretical results.

This letter is organized as follows. In Section II, we describe the system model. In Section III, we study the CPE. In Section IV, we compute the power of the ISI plus ICI as a function of the system parameters. In Section V, the symbol error rate is studied, while numerical results are reported in Section VI. Then, the conclusions follow.

Manuscript received August 8, 2010; revised February 19, 2011; accepted June 14, 2011. The associate editor coordinating the review of this letter and approving it for publication was S. Wei.

The authors are with the University of Udine, Italy (e-mail: {nicola.moret, tonello}@uniud.it).

Part of this work has been presented at the IEEE Sixth International Symposium on Wireless Communication Systems 2009 (ISWCS09), and it has been supported by the European Community's Seventh Framework Programme FP7/2007-2013 under grant agreement no. 213311, project OMEGA-Home Gigabit Networks.

Digital Object Identifier 10.1109/TWC.2011.072511.101422

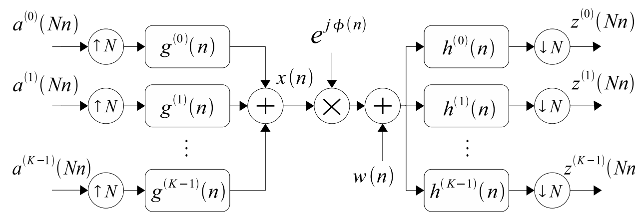

Fig. 1: Filter bank modulation scheme including the phase noise.

II. Filter Bank Modulation Scheme

We consider a FB scheme as depicted in Fig. 1 where the discrete-time transmitted signal at the output of the synthesis FB, $x(n)$, is obtained by the modulation of K data streams at low rate $a^{(k)}(Nn)$, with $k \in \{0, \cdots, K-1\}$, that belong to a constellation signal set, e.g., PSK or QAM. The transmitted signal can be written as

$$x(n) = \sum_{k=0}^{K-1} \sum_{\ell \in \mathbb{Z}} a^{(k)}(N\ell) g^{(k)}(n - N\ell), \qquad (1)$$

where $N \geq K$ is the sample/interpolation factor and $\mathbb{Z}$ in the set of integer numbers. According to (1), the signals $a^{(k)}(Nn)$ are upsampled by a factor N and filtered by the modulated pulses $g^{(k)}(n) = g(n)e^{j\frac{2\pi}{K}kn}$, where $g(n)$ is the prototype pulse. Then, the sub-channel signals are summed and transmitted over the channel.

The phase noise introduces a multiplicative distortion $\omega(n) = e^{j\phi(n)}$ to the transmitted signal $x(n)$, where the random process $\phi(n)$ is the phase noise whose statistical model is defined below. We furthermore consider an ideal propagation media to better understand the impact of the phase noise process on a FB system. The received signal is passed through an analysis FB with pulses $h^{(k)}(n)$. The sub-channel outputs of the FB are sampled by a factor N. If we define the equivalent (time variant) impulse response between the input sub-channel k and the output sub-channel i as $g_{eq}^{(i,k)}(Nm, N\ell) = \sum_n g^{(k)}(n - N\ell)h^{(i)}(Nm - n)\omega(n)$, the analysis FB signal output, for sub-channel i, can be written as

$$\begin{aligned} z^{(i)}(Nm) &= g_{eq}^{(i,i)}(Nm, Nm)\, a^{(i)}(Nm) \\ &\quad + \sum_{\ell \in \mathbb{Z},\, \ell \neq m} a^{(i)}(N\ell) g_{eq}^{(i,i)}(Nm, N\ell) \\ &\quad + \sum_{k=0,\, k\neq i}^{K-1} \sum_{\ell \in \mathbb{Z}} a^{(k)}(N\ell) g_{eq}^{(i,k)}(Nm, N\ell) + w^{(i)}(Nm) \\ &= S^{(i)}(Nm) + I^{(i)}(Nm) + w^{(i)}(Nm), \qquad (2) \end{aligned}$$

where the signal of interest is denoted with $S^{(i)}(Nm)$ (first term in (2)), while the inter-symbol plus inter-channel interference is denoted with $I^{(i)}(Nm)$ (second and third term in (2)). The interference is a function of both the prototype pulse and the phase-noise process. Furthermore, $w^{(i)}(Nm)$ is the additive Gaussian noise contribution.

The phase noise process $\phi(n)$ can be assumed to be a stationary Gaussian process with zero mean and periodic power spectral density (PSD)

$$R_\phi(f) = \sum_{n \in \mathbb{Z}} \hat{R}_\phi(f - n), \qquad (3)$$

$$\hat{R}_\phi(f) = 10^{-c_\phi} + \begin{cases} 10^{-a_\phi} & |f| \leq f_{\phi_1} \\ 10^{-(|f| - f_{\phi_1})\frac{b_\phi}{f_{\phi_2} - f_{\phi_1}} - a_\phi} & |f| \geq f_{\phi_1}, \end{cases}$$

according to the model already used in [7], [11]. This PSD model allows us to describe a wide class of commercial oscillators. The coefficient c_ϕ determines the noise floor, while b_ϕ defines the slope, a_ϕ and f_{ϕ_1} establishes the white phase noise region, and finally f_{ϕ_2} is the frequency where the noise floor is dominant (Fig. 2a). If we assume the PN variance σ_ϕ^2 to be small, i.e., $\sigma_\phi^2 << 1$, the term $\omega(n)$ can be rewritten using Taylor series expansion as

$$\omega(n) = e^{j\phi(n)} \approx 1 + j\phi(n). \qquad (4)$$

With this approximation that we use throughout this letter, $\omega(n)$ can be assumed to be stationary with PSD $R_\omega(f) = \sum_n \delta(f - n) + R_\phi(f)$ and correlation $r_\omega(n_1 - n_2) = E[\omega(n_1)\omega^*(n_2)]$ that is obtained via the inverse Fourier transform of the periodic PSD $R_\omega(f)$. Thus, there is a straightforward relation between the processes $\phi(n)$ and $\omega(n)$.

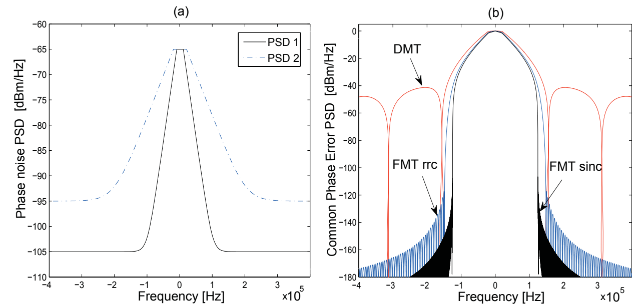

Fig. 2: (a) - Phase noise PSD models with system transmission bandwidth $B = 10\,MHz$. PSD 1 has parameters $f_1 B = 10\ kHz$, $f_2 B = 100\,kHz$, $a = 6.5$, $b = 4$ and $c = 10.5$; PSD 2 has parameters $f_1 B = 20\ kHz$, $f_2 B = 200\ kHz$, $a = 6.5$, $b = 3$ and $c = 9.5$.
(b) - PSD of the CPE considering DMT and FMT, and the PSD 2 model. The parameters are $K = 64$, $N = 80$, and the rrc filter has a roll off factor 0.2 and length $L_g = 12N$.

III. Common Phase Error Analysis

In the signal of interest $S^{(i)}(Nm)$ in (2), the transmitted data symbol $a^{(i)}(Nm)$ is weighted by the factor $g_{eq}^{(i,i)}(Nm, Nm) = \sum_n g(n - Nm)\omega(n)h(Nm - n)$. We denote the phase of this weighting factor with $\Theta(Nm) = \angle(g_{eq}^{(i,i)}(Nm, Nm))$, and we refer to it as *Common Phase Error* (CPE) [7] since it is identical for all the sub-channels. The CPE introduces a random phase rotation on the transmitted symbols. In this section, we analyze the CPE as a function of the prototype pulse deployed in the FB.

Assuming the model in (4) and with $\sum_n g(n)h(-n) = 1$, we can approximate the data symbol weighing factor as

$$g_{eq}^{(i,i)}(Nm, Nm) \approx 1 + j\sum_n g(n - Nm)h(Nm - n)\phi(n). \qquad (5)$$

Furthermore, since $\Theta(Nm) \approx \Im[g_{eq}^{(i,i)}(Nm, Nm)]$ (exploiting the Taylor series expansion of the $arctan(\cdot)$ function), we obtain

$$\Theta(Nm) \approx \sum_{n \in \mathbb{Z}} g(n - Nm)h(Nm - n)\phi(n). \qquad (6)$$

Finally, the weighting factor can be approximated as $g_{eq}^{(i,i)}(Nm, Nm) \approx 1 + j\Theta(Nm) \approx e^{j\Theta(Nm)}$.

Now, if we define $g_-(n) = g(-n)$, the CPE is obtained by the convolution of the PN process with the pulse $g_-(n)\, h(n)$, i.e., $\Theta(Nm) = [(g_-\, h) * \phi]\,(Nm)$, where $*$ denotes convolution. It follows that the PSD of the CPE can be written as

$$\begin{aligned} R_\Theta(f) &= \sum_{n=0}^{N-1} \hat{R}_\Theta(f - \frac{n}{N}), \\ \hat{R}_\Theta(f) &= |(G_- * H)(f)|^2\, R_\phi(f), \qquad (7) \end{aligned}$$

where we denote with $G_-(f)$ and $H(f)$ the discrete time Fourier transform (DTFT) of the pulses $g_-(n)$ and $h(n)$, e.g., $F[h(n)] = H(f) = \sum_n h(n)e^{-j2\pi fn}$.

For certain choices of the prototype pulse, it is possible to derive (7) in closed form. For example, if we consider the DMT system with K sub-channels and with cyclic prefix (CP) of length $N-K$ samples, the synthesis/analysis prototype pulses are $g(n) = \frac{1}{\sqrt{K}} rect(n/N)$ and $h(n) = \frac{1}{\sqrt{K}} rect(-n/K)$, where we have defined the rectangular function as $rect(n/K) = 1$ for $n \in \{0, \cdots, K-1\}$, and as 0 elsewhere. Since $g_{-}(n)h(n) = \frac{1}{K} rect(-n/K)$, and considering that the DTFT of $rect(n/K)$ is equal to $e^{-j\pi f(K-1)} \frac{sin(\pi f K)}{sin(\pi f)}$, $\hat{R}_{\Theta}$ in (7) can be rewritten as

$$\hat{R}_{\Theta}^{DMT}(f) = \left| \frac{1}{K} \frac{sin(\pi f K)}{sin(\pi f)} \right|^2 R_{\phi}(f). \tag{8}$$

Analogously, considering an FMT system deploying a root raised cosine (rrc) prototype pulse [12], with K sub-channels and oversampling factor N, we have that (7) can be written as

$$\hat{R}_{\Theta}^{FMT,rrc}(f) = \left| F[rrc^2\left(\frac{n}{N}\right)] \right| \tag{9}$$

The DTFT of the square of the rrc pulse in (9) cannot be expressed in a closed form except when the roll-off factor is set to 0, i.e., when the rrc pulse corresponds to the sinc pulse defined as $sinc(n) = \frac{sin(\pi n)}{\pi n}$. In such a case the prototype pulses are $g(n) = h(-n) = \frac{1}{\sqrt{N}} sinc(n/N)$. Now, the DTFT of $g_{-}(n)h(n) = \frac{1}{N} sinc^2(n/N)$ is equal to $\sum_k \Lambda(Nf-k)$ where we have defined the triangle function as $\Lambda(f) = 1 - |f|$, if $|f| < 1$, and as 0 elsewhere. Thus, for the FMT system deploying a sinc prototype pulse $\hat{R}_{\Theta}$ in (7) is equal to

$$\hat{R}_{\Theta}^{FMT,sinc}(f) = |\sum_{k \in \mathbb{Z}} \Lambda(Nf-k)|^2 \; R_{\phi}(f). \tag{10}$$

The analysis of (10) reveals that the PSD $\hat{R}_{\Theta}^{FMT,sinc}$ is perfectly set to zero outside the normalized band $2/N$, differently from $\hat{R}_{\Theta}^{DMT}$ in (8) where the white component of the phase noise gives a contribution to the CPE power. In Fig. 2b, we report the PSD of the CPE for both DMT and FMT, and we show that FMT has higher rejection to the CPE due to the sub-channel frequency confinement. As an example, we evaluate the CPE power derived from (7) with $K = \{64, 256, 1024\}$, $N = 5/4K$, and the PSD 2 model of Fig. 2a. The CPE power, in dB, is respectively equal to $\{-16.1, -19.5, -25.2\}$ for DMT, $\{-17.0, -21.2, -27.3\}$ for FMT deploying a rrc pulse with roll-off factor 0.2 and filter length $L_g = 12N$, and $\{-17.4, -21.8, -27.8\}$ for FMT deploying a sinc pulse. The advantage of FMT w.r.t. DMT in terms of coping with the CPE gets larger as the number of sub-channels increases.

IV. Analytical Evaluation of the ISI and ICI Power

We now evaluate the power of the signal of interest and of the interference components defined in (2). We assume the data symbols to be i.i.d. with zero mean, with average power σ_a^2, and the model in (4) for $\omega(n)$ so that the received signal (2) is stationary. Thus, the total average power of the received signal at time instant $Nm = 0$ for sub-channel of index i, reads

$$M_z^{(i)} = \sigma_a^2 \sum_{k=0}^{K-1} \sum_{\ell \in \mathbb{Z}} E[|g_{eq}^{(i,k)}(0, N\ell)|^2]. \tag{11}$$

Since $g_{eq}^{(i,k)}(0, N\ell) = \sum_n g^{(k)}(n - N\ell) h^{(i)}(-n) \omega(n)$, if we define the product filter response $gh^{(i,k)}(N\ell, n) = g^{(k)}(n - N\ell) h^{(i)}(-n)$, we will obtain the following relation

$$E[|g_{eq}^{(i,k)}(0, N\ell)|^2] = \sum_{n_1, n_2 \in \mathbb{Z}} gh^{(i,k)}(N\ell, n_1) r_{\omega}(n_1 - n_2) \times gh^{(i,k)^*}(N\ell, n_2). \tag{12}$$

If we separate the power of the signal of interest from the power of the interference terms, we can write $M_z^{(i)} = M_S + M_I$ where

$$M_S = E[|S^{(i)}(0)|^2] = \sigma_a^2 E[|g_{eq}^{(i,i)}(0,0)|^2] = \sigma_a^2 (1 + \sigma_{\phi}^2) \approx \sigma_a^2 \tag{13}$$

$$M_I = E[|I^{(i)}(0)|^2] = \sigma_a^2 \sum_{\ell \in \mathbb{Z},\, \ell \neq 0} E[|g_{eq}^{(i,i)}(0, N\ell)|^2] + \sigma_a^2 \sum_{k=0,\, k \neq i}^{K-1} \sum_{\ell \in \mathbb{Z}} E[|g_{eq}^{(i,k)}(0, N\ell)|^2]. \tag{14}$$

It should be pointed out that in the presence of phase noise, the DMT system suffers of only inter-channel interference (ICI), while the FMT system is predominantly affected by inter-symbol interference (ISI) due to its frequency confined pulses. Furthermore, given the symmetry of the prototype pulses and of the phase noise PSD, the power of the signal of interest and of the interference is the same for all sub-channel indices. We can therefore define the average sub-channel signal-to-noise plus interference ratio as $SINR = M_S/(M_I + M_w)$ where $M_w = \sigma_w^2$ is the power of the additive noise component in the sub-channel.

V. Error Rate Analysis in the Presence of Phase Noise

In this section we discuss the symbol error rate (SER) assuming two different types of receivers. Firstly, we consider a *non-coherent receiver* (NCR) that assumes no knowledge of the data symbol weighting factor, and uses the following decision metric for sub-channel i

$$\hat{a}^{(i)}(Nm) = \arg\min_{a \in A} ||z^{(i)}(Nm) - a||^2, \tag{15}$$

where the symbol alphabet is denoted with A.

Secondly, we consider a one-tap equalizer where, on the contrary, we take into account the perfect knowledge of the data symbol weighting factor using the decision metric

$$\hat{a}^{(i)}(Nm) = \arg\min_{a \in A} ||z^{(i)}(Nm) - g_{eq}^{(i,i)}(Nm, Nm) a||^2. \tag{16}$$

We refer to this receiver as the *one-tap coherent receiver* (CR). The weighting factor (related to the CPE) can be in practice estimated, for instance, with the method proposed in [7] for DMT.

To proceed, the received signal can be approximated as $z^{(i)}(Nm) \approx a^{(i)}(Nm) e^{j\Theta(Nm)} + I^{(i)}(Nm) + w^{(i)}(Nm)$, since $g_{eq}^{(i,i)}(Nm, Nm) \approx e^{j\Theta(Nm)}$ as discussed in Section III. Furthermore, we assume the interference to be Gaussian distributed, which holds true for a large number of interference components. These assumptions allow us to obtain quasi-closed form expressions for the SER of M-PSK and M-QAM that are in good agreement with simulation results.

A. Symbol Error Rate Analysis for the Non-Coherent Receiver (NCR)

1) SER conditioned by the CPE for M-PSK with the NCR As it is proved in the Appendix A, for 4-PSK modulation the SER conditioned by Θ with the NCR, under the Gaussian approximation for the interference, is given by

$$P_e^{(4PSK)}(\Theta)=1-\left(1-Q\left(\sqrt{SINR}\,sin(\frac{\pi}{4}+\Theta)\right)\right.\\ \left.\times\left(1-Q\left(\sqrt{SINR}\,cos(\frac{\pi}{4}+\Theta)\right)\right)\right), \quad (17)$$

where $Q(x) = 1 - \Phi(x)$ and $\Phi(x)$ is the the normalized Gaussian cumulative distribution function.

For M-PSK modulation, with $M > 4$, the conditional SER with the NCR can be approximated as (see the Appendix A).

$$P_e^{(MPSK)}(\Theta) \approx Q\left(\sqrt{SINR}\,sin(\frac{\pi}{M}-\Theta)\right)\\ +Q\left(\sqrt{SINR}\,sin(\frac{\pi}{M}+\Theta)\right). \quad (18)$$

2) SER conditioned by the CPE for M-QAM with the NCR Assuming M-QAM square constellations with data symbols $c_{i,k} = (2i - 1 - \sqrt{M}) + j(2k - 1 - \sqrt{M})$ with $(i, k) \in \{1, \cdots, \sqrt{M}\}$ and the NCR, the probability to correctly receive a symbol, conditioned by the CPE Θ, is (see the Appendix B)

$$\begin{aligned} P_c^{(QAM)}(\Theta) = &\sum_{i=2}^{S}\sum_{k=2}^{S}\frac{4}{M}\left[\Phi(\lambda R_{i,k}) - Q(\lambda L_{i,k})\right] \\ &\times\left[\Phi(\lambda U_{i,k}) - Q(\lambda D_{i,k})\right] \\ &+\sum_{i=2}^{S}\frac{4}{M}\Phi(\lambda U_{i,1})\left[\Phi(\lambda R_{i,1}) - Q(\lambda L_{i,1})\right] \\ &+\sum_{k=2}^{S}\frac{4}{M}\Phi(\lambda R_{1,k})\left[\Phi(\lambda U_{1,k}) - Q(\lambda D_{1,k})\right] \\ &+\frac{4}{M}\Phi(\lambda U_{1,1})\Phi(\lambda R_{1,1}), \end{aligned} \quad (19)$$

where $S = \sqrt{M}/2$, $\lambda = \sqrt{\frac{3\,SINR}{2\,(M-1)}}$, and we have defined $R_{i,k} = \left|\Re\left[c_{i,k}e^{j\Theta} - (c_{i,k}+1)\right]\right|$, $L_{i,k} = \left|\Re\left[c_{i,k}e^{j\Theta} - (c_{i,k}-1)\right]\right|$, $U_{i,k} = \left|\Im\left[c_{i,k}e^{j\Theta} - (c_{i,k}+j)\right]\right|$, $D_{i,k} = \left|\Im\left[c_{i,k}e^{j\Theta} - (c_{i,k}-j)\right]\right|$. The conditional SER for M-QAM is therefore $P_e^{(QAM)}(\Theta) = 1 - P_c^{(QAM)}(\Theta)$.

1) Average SER with the NCR: The average SER with the NCR is obtained from the conditional SER of M-PSK or M-QAM as follows

$$P_e = \int_{-\infty}^{+\infty} P_e(\theta) f_\Theta(\theta)\, d\theta, \quad (20)$$

where $f_\Theta(\theta)$ is the probability density function of Θ. Since Θ is a sum of several Gaussian components, as shown by (6), we assume it to be Gaussian distributed with zero mean and variance $\sigma_\Theta^2 = \int_{-1/2N}^{1/2N} R_\Theta(f)df$, where $1/N$ is the normalized sub-channel transmission band. The average SER in (20), then is obtained via numerical integration.

B. Symbol Error Rate Analysis for the One-Tap Coherent Receiver (CR)

We now consider the CR decision metric. Since in Section III we have shown that the signal weighting factor can be approximated as $g_{eq}^{(i,i)}(Nm, Nm) \approx e^{j\Theta(Nm)}$ according to the model in (4), then its amplitude is constant, i.e., $|g_{eq}^{(i,i)}(Nm, Nm)| \approx 1$, and the coherent receiver perfectly compensates the phase of the signal of interest. Therefore, the average SER can be simply computed using conventional formulas for the SER in AWGN [12] provided that we approximate the interference as a Gaussian process and we use the SINR defined in Section IV.

VI. Numerical Results

We compare the DMT and the FMT system in the presence of phase noise in terms of SER as a function of the $SNR = \sigma_a^2/\sigma_w^2$. We consider 4-PSK, 8-PSK, and 64-QAM constellations. We assume an overall transmission bandwidth equal to $B = 10\,MHz$, $K = 64$ sub-channels, and an interpolation/sampling factor $N = 80$. The pulses used in DMT are $g(n) = \frac{1}{\sqrt{K}}rect(n/N)$ and $h(n) = \frac{1}{\sqrt{K}}rect(-n/K)$. The FMT system deploys a root-raised-cosine pulse ($g(n) = h(-n) = rrc(n/N)$) with roll-off factor 0.2 and number of coefficients $L_g = 12N$. The two systems have identical data rate.

Fig. 3 reports the Montecarlo simulation results and the theoretical SER curves using the NCR decision metric and with the phase noise PSD 1 or PSD 2 of Fig. 2a. In Fig. 4, we consider the CR with the same PN PSD models. The results show that the theoretical performance curves are close to those obtained via simulations, which proves that the proposed approximation for the received signal, including the Gaussian assumption for the ISI/ICI, allows us to predict the SER. Phase noise introduces a SER degradation which is more pronounced for high order constellations, and clearly, for the PSD 2 that is associated to heavier PN. Furthermore, the FMT system has better performance compared to the DMT system, i.e., it has higher capability to cope with the PN, for all the PN PSD models considered, due to its higher sub-channel spectral containment. Furthermore, DMT with cyclic prefix has a small SNR loss since the receiver FB is not matched to the transmitter FB. Fig. 4 shows that the CR can correct the distortion due to the CPE and therefore it yields better performance than the NCR which is close to the performance in the absence of PN. Although both systems suffer of the presence of interference components, in FMT the interference power is dominated by the ISI, while in DMT by the ICI. Therefore, sub-channel equalization can in principle be useful to improve the SER performance in FMT .

VII. Conclusion

We have analyzed the effect of phase noise on filter bank transmission systems. In particular, we have considered the DMT and the FMT systems and reported a general analysis of the distortion due to the CPE and the interferences using a stationary model for the PN impairment process. We have considered a non-coherent and a one-tap coherent receiver where the first receiver assumes no knowledge of the CPE, while the second receiver assumes it perfectly known. The theoretical and simulation results are in good agreement and show that FMT, with a root-raised-cosine prototype pulse, has better performance than DMT with both receivers. The

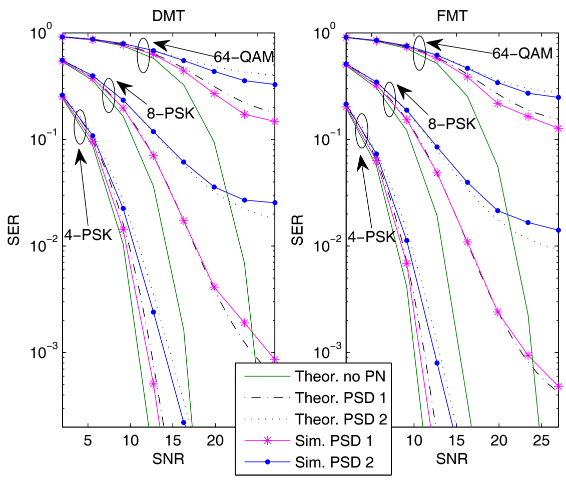

Fig. 3: SER for DMT and FMT with the non-coherent receiver, with $B = 10\ MHz$, $K = 64$ and $N = 80$ ($CP = 16$). Both simulation and theoretical results, from (18) and (19), are shown.

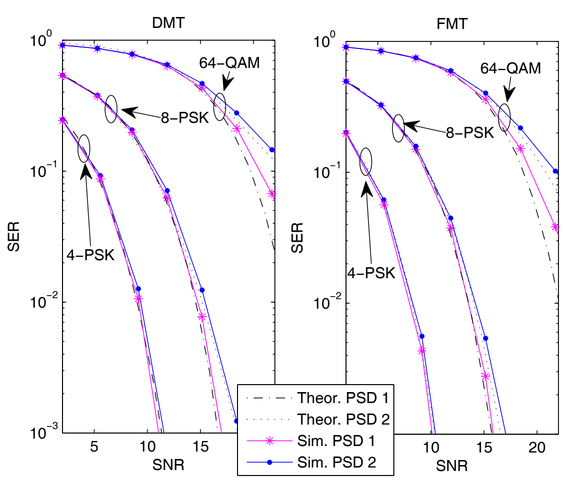

Fig. 4: SER for DMT and FMT with the single tap coherent receiver, with $B = 10\ MHz$, $K = 64$ and $N = 80$ ($CP = 16$). Both simulation and theoretical results are shown.

compensation of the CPE yields significant improvements w.r.t. the non-coherent receiver.

Appendix A
Probability of Error for 4-PSK and M-PSK with the NCR

We consider 4-PSK modulation having symbols $c_k = e^{j(\pi/4+k\pi/2)}$ with $k \in \{0, 1, 2, 3\}$. The received signal (2) can be simply written as $z = ae^{j\Theta} + \eta$, since $g_{eq}^{(i,i)} \approx e^{j\Theta}$, where $a \in \{c_0, \cdots, c_3\}$, Θ is defined in (6), and η, that comprises ISI plus ICI and noise, is modeled as a stationary Gaussian process with variance σ_η^2. The SER is $P_e^{(4PSK)}(\Theta) = 1 - P_c^{(4PSK)}(\Theta)$, where $P_c^{(4PSK)}(\Theta)$ is the correct decision probability with the NCR conditioned by the CPE. It is equal to $P_c^{(4PSK)}(\Theta) = 1/4\sum_{k=0}^{3} P_c^{(4PSK)}(\Theta, c_k)$ where $P_c^{(4PSK)}(\Theta, c_k)$ is the correct decision probability conditioned on the transmission of the symbol c_k.

We now consider the transmission of symbol $a = c_0 = e^{j\pi/4}$. It is correctly received if $\Re[\eta_k] > -d_{1,0}$ and $\Im[\eta_k] > -d_{2,0}$ where $d_{1,0} = |\Re[c_0 e^{j\Theta}]| = cos(\pi/4 + \Theta)$ and $d_{2,0} = |\Im[c_0 e^{j\Theta}]| = sin(\pi/4 + \Theta)$ are the minimum distances between $c_0 e^{j\Theta}$ and the boundaries of the decision region (axes). Thus, $P_c^{(4PSK)}(\Theta, c_0) = (1 - Q(d_{1,0}/\sigma_\eta)(1 - Q(d_{2,0}/\sigma_\eta))$. By symmetry, the same argument is valid if the other symbols $\{c_1, c_2, c_3\}$ are transmitted. Finally, we obtain that $P_c^{(4PSK)}(\Theta) = (1 - Q(d_{1,0}/\sigma_\eta))((1 - Q(d_{2,0}/\sigma_\eta))$.

Considering M-PSK modulation, with $M > 4$ and symbols $c_k = e^{j(\pi/M+2k\pi/M)}$, $k \in \{0, \cdots, M-1\}$, we use the nearest neighbor symbol approximation. The minimum distances between the rotated symbol $ae^{j\Theta}$ and the adjacent boundaries of the decision region are $d_1 = sin(\pi/M - \Theta)$ and $d_2 = sin(\pi/M + \Theta)$. Thus, we can use the approximation $P_e^{(MPSK)}(\Theta) \approx Q(d_1/\sigma_\eta) + Q(d_2/\sigma_\eta)$, which proves (18).

Appendix B
Probability of Error for M-QAM with the NCR

In M-QAM modulation with square constellations, the symbols are defined as $c_{i,k} = (2i-1-\sqrt{M}) + j(2k-1-\sqrt{M})$ with $(i, k) \in \{1, \cdots, \sqrt{M}\}$. To obtain the SER with the NCR conditioned on the CPE, we start from the signal model $z = ae^{j\Theta} + \eta$ as in Appendix A. Furthermore, with the non-coherent metric in (16) we can identify three shapes of decision region depending on where the symbol is located: symbol in the constellation corner, symbol with three minimum distance neighbors, and symbol with four minimum distance neighbors. Furthermore, let us consider to transmit the symbol $a = c_{i,k}$, then we define $R_{i,k} = \left|\Re[c_{i,k}e^{j\Theta} - (c_{i,k} + 1)]\right|$ as the minimum distance between the symbol affected by the CPE and the right boundary of the decision region associated to $c_{i,k}$. Analogously, we define $L_{i,k} = \left|\Re[c_{i,k}e^{j\Theta} - (c_{i,k} - 1)]\right|$, $U_{i,k} = \left|\Im[c_{i,k}e^{j\Theta} - (c_{i,k} + j)]\right|$, and $D_{i,k} = \left|\Im[c_{i,k}e^{j\Theta} - (c_{i,k} - j)]\right|$ as the minimum distances between the symbol affected by the CPE and, respectively, the left, the upper and the lower boundaries of the decision region.

Now, exploiting the symmetry of the problem, we need to compute the conditional probability of correct detection $P_c^{(QAM)}(\Theta, a = c_{i,k})$ only for the symbols $c_{i,k}$ with $i \in \{1, \cdots, \sqrt{M}/2\}$ and $k \in \{1, \cdots, \sqrt{M}/2\}$ (i.e. the symbols that are located on the lower-left quadrant of the Cartesian plane). Therefore, if the symbol belongs to the lower-left corner ($i = k = 1$) the probability of a correct decision is $P_c^{(QAM)}(\Theta, c_{1,1}) = \Phi(\frac{U_{1,1}}{\sigma_\eta})\Phi(\frac{R_{1,1}}{\sigma_\eta})$. For the symbols $c_{i,k}$ with $k = 1$, $i \in \{2, \cdots, \sqrt{M}/2\}$ we obtain $P_c^{(QAM)}(\Theta, c_{i,1}) = \Phi(\frac{U_{i,1}}{\sigma_\eta})\left(\Phi(\frac{R_{i,1}}{\sigma_\eta}) - Q(\frac{L_{i,1}}{\sigma_\eta})\right)$. For the symbols $c_{i,k}$ with $i = 1$, $k \in \{2, \cdots, \sqrt{M}/2\}$) we obtain $P_c^{(QAM)}(\Theta, c_{1,k}) = \Phi(\frac{R_{1,k}}{\sigma_\eta})\left(\Phi(\frac{U_{1,k}}{\sigma_\eta}) - Q(\frac{D_{1,k}}{\sigma_\eta})\right)$. Finally, for the symbols $c_{i,k}$ with $i \in \{2, \cdots, \sqrt{M}/2\}$, $k \in \{2, \cdots, \sqrt{M}/2\}$) we have that $P_c^{(QAM)}(\Theta, c_{i,k}) = \left(\Phi(\frac{R_{i,k}}{\sigma_\eta}) - Q(\frac{L_{i,k}}{\sigma_\eta})\right)\left(\Phi(\frac{U_{i,k}}{\sigma_\eta}) - Q(\frac{D_{i,k}}{\sigma_\eta})\right)$.

If we now define $S = \sqrt{M}/2$, we obtain

$$P_c^{(QAM)}(\Theta) = \\ = \sum_{i=2}^{S}\sum_{k=2}^{S}\frac{4}{M}P_c^{(QAM)}(\Theta, c_{i,k}) + \sum_{i=2}^{S}\frac{4}{M}P_c^{(QAM)}(\Theta, c_{i,1}) \\ + \sum_{k=2}^{S}\frac{4}{M}P_c^{(QAM)}(\Theta, c_{1,k}) + \frac{4}{M}P_c^{(QAM)}(\Theta, c_{1,1}). \tag{21}$$

Since the average constellation energy is $\sigma_a^2 = 2(M-1)/3$, the signal to noise plus interference ratio can be written as $SINR = \sigma_a^2/\sigma_\eta^2$ with $\sigma_\eta^2 = E[|\eta|^2]$ (see the Appendix A). Thus, we obtain (19) from (21).

REFERENCES

[1] G. Cherubini, E. Eleftheriou, and S. Olcer, “Filtered multitone modulation for very high-speed digital subscribe lines," *IEEE J. Sel. Areas Commun.*, pp. 1016–1028, June 2002.

[2] A. M. Tonello, “Performance limits for filtered multitone modulation in fading channels," *IEEE Trans. Wireless Commun.*, vol. 4, pp. 2121–2135, Sep. 2005.

[3] S. Weinstein and P. Ebert, “Data transmission by frequency-division multiplexing using the discrete Fourier transform," *IEEE Trans. Commun. Technol.*, vol. 19, pp. 628–634, Oct. 1971.

[4] B. Borna and T. Davidson, “Efficient design of FMT systems," *IEEE Trans. Commun.*, vol. 54, pp. 794–797, May 2006.

[5] N. Moret and A. M. Tonello, “Design of orthogonal filtered multitone modulation systems and comparison among efficient realizations," *EURASIP J. Advanced Signal Process.*, 2010.

[6] A. M. Tonello and F. Pecile, “Analytical results about the robustness of FMT modulation with several prototype pulses in time-frequency selective fading channels," *IEEE Trans. Wireless Commun.*, vol. 7, pp. 1634–1645, May 2008.

[7] P. Robertson and S. Kaiser, “Analysis of the effect of phase-noise in orthogonal frequency division multiplex (OFDM) system," in *Proc. IEEE ICC*, pp. 1652–1657, June 1995.

[8] L. Piazzo and P. Mandarini, “Analysis of phase noise effects in ODFM modems," *IEEE Trans. Commun.*, vol. 50, pp. 1696–1705, Oct. 2002.

[9] D. D. Lin, Y. Zhao, and T. J. Lim, “OFDM phase noise cancellation via approximate probabilistic inference," in *Proc. IEEE Wireless Commun. Netw. Conf.*, vol. 1, pp. 27–32, 2005.

[10] N. Benvenuto, G. Cherubini, and L. Tomba, “Achievable bit rates of DMT and FMT systems in the presence of phase noise and multipath," in *Proc. Veh. Technol. Conf. (VTC 2000-Spring)*.

[11] A. Assalini, S. Pupolin, and A. M. Tonello, “Analysis of the effect of phase noise in filtered multitone (FMT) modulated system," in *Proc. IEEE Globecom*, pp. 3541–3545, Nov. 2004.

[12] J. Proakis, *Digital Communications*, 4th edition. McGraw-Hill, 1995.